PCCP

Self-motion of a camphoric acid boat sensitive to the chemical environment

Yuko Hayashima,[a] Masaharu Nagayama,[b] Yukie Doi,[a] Satoshi Nakata,*[a] Maya Kimura[c] and Masayasu Iida[c]

[a] *Department of Chemistry, Nara University of Education, Takabatake-cho, Nara, 630-8528, Japan. E-mail: nakatas@nara-edu.ac.jp*
[b] *Research Institute for Mathematical Sciences, Kyoto University, Kyoto, 606-8502, Japan*
[c] *Department of Chemistry, Nara Women's University, Kitauoya-nishi-machi, Nara City, 630-8506, Japan*

Received 25th September 2001, Accepted 9th January 2002
First published as an Advance Article on the web 15 March 2002

As a simple example of an autonomous motor, the characteristic patterns in the self-motion of a camphoric acid boat depending on the chemical environment were investigated at the air/aqueous interface. The uniform motion of a camphoric acid boat changed to intermittent motion and its period increased depending on the concentration of phosphate ions. The nature of the self-motion changed reversibly with the addition of chemical stimuli to the air/aqueous interface. The camphoric acid layer adsorbed on a mica surface was observed by atomic force microscopy (AFM) to investigate how the microscopic state of the camphoric acid layer varied with pH. The nature of the self-motion was reproduced by a numerical calculation in relation to the surface tension, which depends on the surface concentration of the camphoric acid layer.

1. Introduction

Studies of artificial motors which mimic biological ones are important not only to understand chemo-mechanical transduction in biological systems but also to create novel artificial motors which adapt to the environment. All motor organs or organelles in living organisms work through the dissipation of chemical energy under almost isothermal and non-equilibrium conditions. Several artificial systems which exhibit self-motion under conditions of chemical non-equilibrium have been studied experimentally[1–16] and theoretically[17–22] under almost isothermal conditions.

More than a century ago, the self-motion of small camphor scrapings floating on water was explained by Van der Mensbrugghe as being due to the diminished surface tension of water. Subsequently, Rayleigh studied the retarding effect of contaminating oily substances on the self-motion of a camphor scraping.[23]

Recently, we reported that the nature of the self-motion of a camphor scraping changes depending on both internal conditions (*e.g.*, scraping morphology and chemical structure of a camphor derivative) and external conditions (*e.g.*, temperature, surface tension, and the shape of the cell) and that the essential features of self-motion could be reproduced by a computer simulation.[24–29] In addition, we reported that the mode of self-motion of a camphoric acid scraping changes depending on the pH of the aqueous phase (uniform motion at an acidic pH, intermittent motion at a neutral pH, and no motion at an alkaline pH).[30–32] However, how the mode of self-motion changes with pH has not yet been clarified.

In this paper, the self-motion of a camphoric acid boat was found to be sensitive to the chemical environment, *i.e.*, concentration of the phosphate buffer solution and the presence of chemical stimuli. The camphoric acid layer adsorbed on a mica surface was imaged by AFM to investigate how the microscopic state of the camphoric acid layer varied with pH. These results are discussed in relation to the mechanism of the characteristic self-motion depending on pH. The nature of self-motion was reproduced by a numerical calculation in relation to the surface tension, which depends on the surface concentration of the camphoric acid layer.

2. Experimental

Camphoric acid and other chemicals were obtained from Wako Chemicals (Kyoto, Japan). Water was first distilled and then purified with a Millipore Milli-Q filtering system (pH of the obtained water: 6.3, resistance of the water: >20 MΩ). The following phosphate buffer solutions (PBS) were used as the aqueous phase: 0.2000 mol l^{-1} KH_2PO_4 (PBS4), 0.1899 mol l^{-1} KH_2PO_4 + 0.0030 mol l^{-1} Na_2HPO_4 (PBS5), 0.0346 mol l^{-1} KH_2PO_4 + 0.0553 mol l^{-1} Na_2HPO_4 (PBS7), 0.0628 mol l^{-1} Na_2HPO_4 + 0.0020 mol l^{-1} Na_3PO_4 (PBS10), 0.0333 mol l^{-1} Na_3PO_4 (PBS12), 0.0173 mol l^{-1} KH_2PO_4 + 0.0277 mol l^{-1} Na_2HPO_4 (PBS7-01), and 0.0692 mol l^{-1} KH_2PO_4 + 0.1106 mol l^{-1} Na_2HPO_4 (PBS7-04). PBS4, PBS5, PBS7, PBS10, and PBS12 were buffered at pH 4.2, 5.1, 7.0, 10.0, and 11.9, respectively, and their ionic strengths were 0.2. The ionic strengths of PBS7-01 and PBS7-04 were 0.1 and 0.4.

A camphoric acid scraping (diameter: *ca.* 1.0 mm), which was connected to the back of a polyester plastic boat (thickness: 0.1 mm), was floated on an aqueous phase (2 ml) in a circular route (inner diameter: 40 mm, width: 5 mm, depth: 2 mm) to simplify the analysis of the motion by control of its direction. At this stage, the camphoric acid scraping without connection to the boat was partly in contact with the water surface and the camphoric acid boat moved in one direction around the route. To obtain high reproducibility for the phenomenon, very similar camphoric acid boats (mass: 3 mg) were prepared for each experiment, *i.e.*, the size and shape of the

 DOI: 10.1039/b108686c

scraping and how the scraping was attached to the boat were almost the same.

The movement of the camphoric acid scraping was monitored with a digital video camera (SONY DCR-VX700) and recorded on videotape at 293 ± 1 K. The two-dimensional position of the camphoric acid and the center of gravity for rotation were measured using a digitizer. The minimum time resolution was 1/30 s. The AFM system used in this study was a commercial microscope (Nanoscope IIIa, Digital Instruments, Santa Barbara, CA). A crystal silicon cantilever (length: 125 mm, resonant frequency: 324–382 kHz) with tapping mode was scanned over the sample in pure air at room temperature. The surface tension on the aqueous surface was measured independently of the motion of the camphoric acid boat by the standard Wilhelmy method, where a platinum ring (diameter: 10 mm) was used as the Wilhelmy plate. The pH in the bulk phase was measured with a pH meter (Toko Co., TP-1000, Japan), with stirring and independently of the motion of the camphoric acid boat. The pH around the aqueous surface was measured with a pH meter (Horiba, twin pH, Japan). Here, 200 μl around the aqueous surface was pipetted as a sample after removal of the camphoric acid boat.

3. Results

3.1. Effect of PBS concentration

Fig. 1 shows the time variation of the velocity of a camphoric acid boat on PBS at pH 7.0 with different concentrations. When the ionic strength was zero, the camphoric acid boat showed uniform motion (Fig. 1(a)). When the initial value of the ionic strength of the aqueous phase was between 0.05 and 0.2, the velocity of the uniform motion fluctuated and the uniform motion changed to intermittent motion depending on the initial concentration (Fig. 1(b)). When the ionic strength was greater than 0.2, periodic intermittent motion was clearly observed (Fig. 1(c)) and the period and resting time of the intermittence increased with the ionic strength (Fig. 1(d)). After movement of the camphoric acid boat for 2 min, the pH around the aqueous surface for Fig. 1(a), (b), (c), and (d) was 4.2, 6.7, 6.8, and 6.9, respectively.

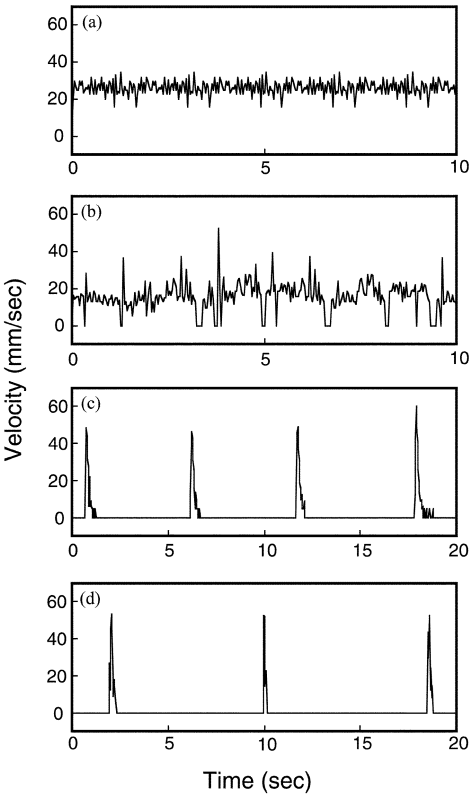

Fig. 1 Time variation of the velocity of a camphoric acid boat on a phosphate aqueous solution with different ionic strengths ((a) 0 (pure water), (b) 0.1(PBS-01), (c) 0.2 (PBS7), and (d) 0.4(PBS-04)).

3.2. Dependence of the surface tension and pH on the concentration of camphoric acid in the aqueous phase

To clarify the mechanism of the mode-change in self-motion, the surface tension and pH were measured depending on the concentration of camphoric acid in the phosphate aqueous phase (Fig. 2). In Fig. 2(a), the surface tension clearly decreased with increasing concentration of camphoric acid, while the pH decreased only slightly. In Fig. 2(b) and (c), the pH decreased depending on the concentration of the camphoric acid. On the other hand, the surface tension did not change above pH 6 (or up to 20 mM for PBS7 and 35 mM for PBS10), but markedly decreased below pH 6 (or above these concentrations of camphoric acid). In Fig. 2(d), the surface tension was almost constant, but the pH decreased depending on the concentration of camphoric acid. Fig. 3 shows the concentration dependences of three camphoric acid molecules ($R(COOH)_2$, $R(COOH)COO^-$, $R(COO^-)_2$, where $R = C_8H_{14}$) when $R(COOH)_2$ molecules were dissolved in the phosphate aqueous solutions. The ratio of the three states of camphoric acid changed differently depending on the pH of the PBS.

3.3. AFM image of the camphoric acid layer depending on the pH and the concentration of the camphoric acid aqueous solution

Although observation of the distribution of the camphoric acid layer is important for understanding the mechanism of self-motion, we have not yet been successful. To observe the condition of the camphoric acid layer, albeit indirectly, an adsorbate on a mica surface was observed with AFM, as shown in Fig. 4. In PBS10 at 20 mM, aggregates of camphoric acid molecules with a spherical shape were observed (Fig. 4(b)). In PBS10 at 60 mM, larger aggregates of camphoric acid molecules with a characteristic shape covered the mica surface (Fig. 4(c)). The amount and state of the adsorbed camphoric acid molecules in Fig. 4(c) were quite different from those in Fig. 4(b), although the concentration in Fig. 4(c) was three times that in Fig. 4(b). The image in Fig. 4(d) was clearly different than that in Fig. 4(c), even with the same concentration of camphoric acid.

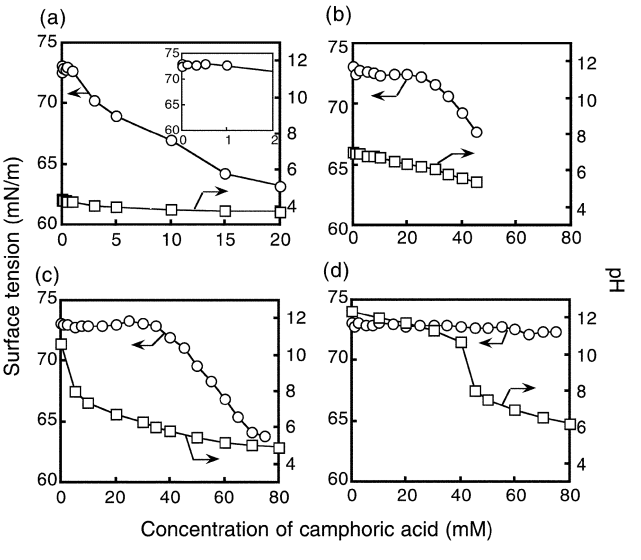

Fig. 2 Dependence of the surface tension (open circle) and pH (open square) on the concentration of camphoric acid dissolved in (a) PBS4, (b) PBS7, (c) PBS10, and (d) PBS12.

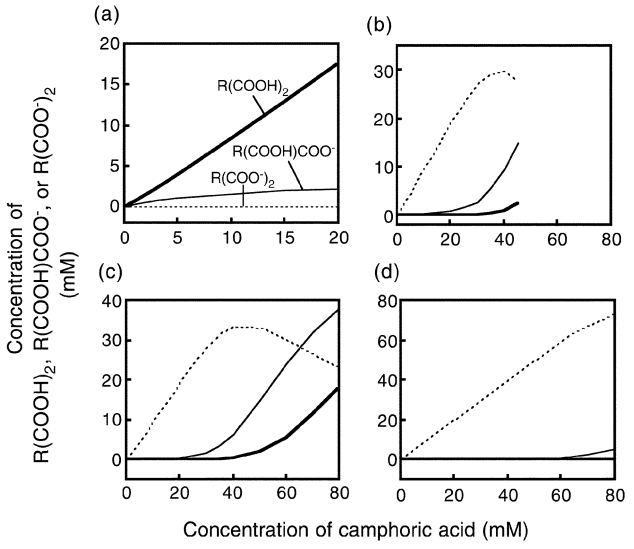

Fig. 3 Concentrations of $R(COOH)_2$, $R(COOH)COO^-$, and $R(COO^-)_2$ (where $R = C_8H_{14}$) when camphoric acid, $R(COOH)_2$, was dissolved in (a) PBS4, (b) PBS7, (c) PBS10, and (d) PBS12. The data in (a), (b), (c), and (d) correspond to those in Fig. 2(a), (b), (c), and (d), respectively, and the individual concentrations for the three states were obtained from pH values in Fig. 2 and pK_{a1} (=4.57) and pK_{a2} (=5.10) for camphoric acid (see Appendix).

3.4. Self-motion of a camphoric acid boat sensitive to chemical stimuli

Fig. 5 shows the time variation of the velocity of a camphoric acid boat on PBS when a chemical stimulus was added to the aqueous solution. In Fig. 5(a), uniform motion was produced as the initial condition without an additive. When NH_3 vapor was applied to the aqueous surface, the uniform motion changed to intermittent motion. In Fig. 5(b), intermittent motion was produced as the initial condition without an additive.

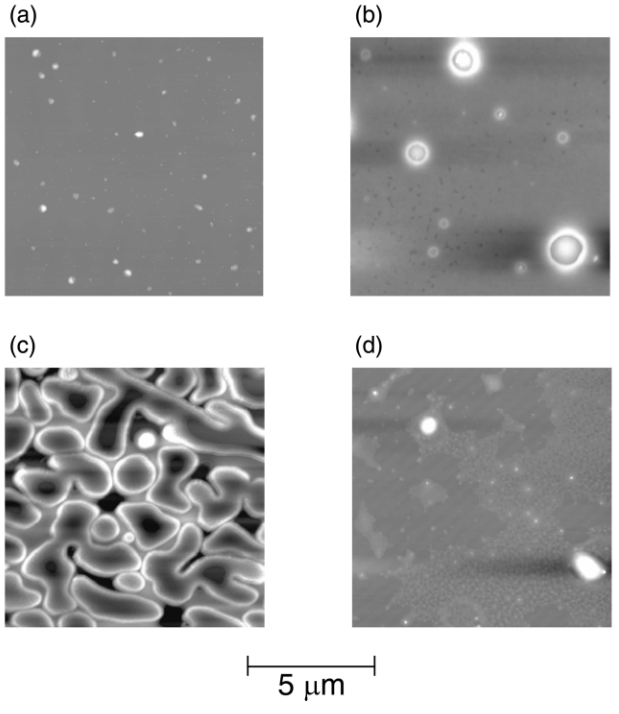

Fig. 4 AFM images (10×10×0.2 μm) for mica surfaces that were in contact with the surface of the different camphoric acid solutions using a horizontal-lifting method. (a) PBS10 without camphoric acid, (b) 20 mM camphoric acid dissolved in PBS10, (c) 60 mM camphoric acid dissolved in PBS10, and (d) 60 mM camphoric acid dissolved in PBS12.

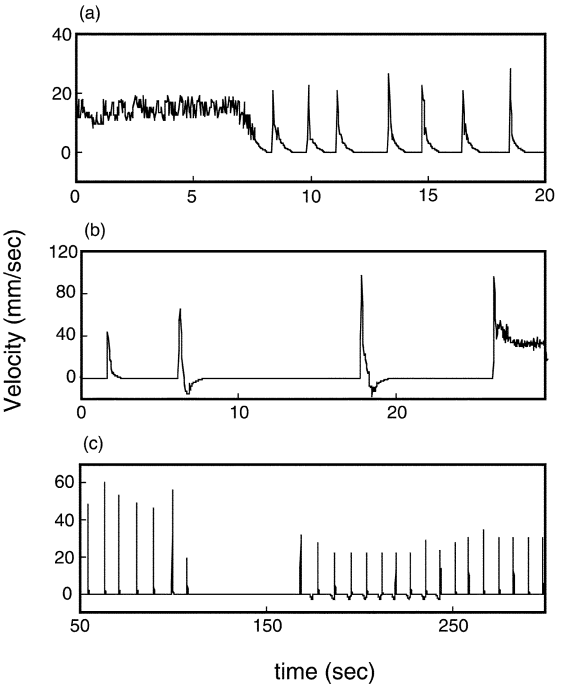

Fig. 5 Time variation of the velocity of the camphoric acid boat, $((dx/dt)^2+(dy/dt)^2)^{1/2}$. (a) NH_3 vapor was applied to the aqueous surface (PBS5) at $t = 5.0$. (b) HCl vapor was applied to the aqueous surface (PBS7) at $t = 5.0$. (c) (i) NH_3 vapor was applied to the aqueous surface (PBS7) at $t = 100$, (ii) the NH_3 vapor was removed and HCl vapor was applied at $t = 150$, and (iii) HCl vapor was removed at $t = 220$. A cotton cloth immersed in a chemical stimulus (6mol l^{-1} NH_3 or 10 mol l^{-1} HCl) was placed near or removed from the surface of PBS (minimum distance between the tip and the PBS surface: *ca.* 5 mm, distance between the tip and boat at the addition of each stimulus: *ca.* 20 mm before the boat passes under the tip). Here, the directional motion of the plastic boat without camphoric acid was defined as the positive velocity.

When the camphoric acid boat had twice passed through the area where HCl vapor was applied to the aqueous surface, intermittent motion changed to uniform motion, including backward motion (note the existence of negative velocity). In Fig. 5(c), intermittent motion immediately changed to no motion when NH_3 vapor was applied to the aqueous surface. When the NH_3 vapor was removed from the aqueous surface and replaced by HCl vapor, no motion changed to intermittent motion, including backward motion. When the HCl vapor was removed from the aqueous surface, intermittent motion without backward motion was observed.

The measurement of pH at the aqueous surface has not yet been successful in our present study since the bulk phase is partly contained in the sampling. Therefore, we used a Bromothymol Blue indicator to check the pH at the aqueous surface on addition of a chemical stimulus. Under similar conditions to those in Fig. 5(a) but without a camphoric acid boat, the color around the aqueous phase changed from yellow to green on addition of NH_3. For Fig. 5(b), the color changed from green to yellow-green on addition of HCl. For Fig. 5(c), the color changed to from green to blue with the addition of NH_3, and to blue-green with the addition of HCl, and was little changed to green after removal of the HCl.

4. Discussion

4.1. Mechanism of the mode-change in self-motion in response to the chemical environment

The effect of the ionic strength suggests that phosphate ions play a role in the formation and deformation of the camphoric

acid layer that develops on the aqueous surface from the solid. The uniform motion at $\mu = 0$ (Fig. 1(a)) is due to the successive formation of a surface active camphoric acid layer as the driving force, since camphoric acid is slightly soluble in water. The intermittent motion at $\mu > 0.2$ may be induced by the following mechanisms, as shown schematically in Fig. 6. The camphoric acid molecules ($R(COOH)_2$, where $R = C_8H_{14}$), which develop from the camphoric acid scraping, are ionized with phosphate ions ($R(COOH)_2 + 2HPO_4^{2-} \rightarrow R(COO^-)_2 + 2H_2PO_4^-$) in the sub-phase (around the air/water interface) (Step I). The completely ionized camphoric acid molecules ($R(COO^-)_2$) are surface inactive, therefore the boat does not move. However, the buffer function decreases due to the decrease in the subphase concentration of HPO_4^{2-}, and a surface active camphoric acid layer then accumulates at the aqueous surface (Step II). Therefore, the camphoric acid boat moves to another location without a camphoric acid layer and with sufficient HPO_4^{2-}. Thus, intermittent motion is generated by repetition of Steps I and II. The increase in the resting time of the intermittence with the increase in the ionic strength of the phosphate solution (Fig. 1) suggests that the concentration of HPO_4^{2-} is sufficient in the resting state but insufficient in the moving state to play the role of a buffer solution.

Fig. 2 and 3 suggest that $R(COOH)_2$ is surface active and plays an important role as the driving force in self-motion, since the surface tension decreased when the concentration of $R(COOH)_2$ increased. On the other hand, $R(COO^-)_2$ is surface inactive (Fig. 2(d) and 3(d)). $R(COOH)COO^-$ may also play a role as a surface active substance (Fig. 2(c) and 3(c)). According to the Langmuir adsorption isotherm,[33] the adsorption ratio among three states, $\theta_\alpha : \theta_\beta : \theta_\gamma$, is determined by $K_\alpha C_\alpha : K_\beta C_\beta : K_\gamma C_\gamma$, where α denotes state R–$(COOH)_2$, β is the state R–(COOH)(COO^-), and γ is the state R–$(COO^-)_2$, , and K_{1x} is the equilibrium constant for the surface adsorption/desorption of ($K_{1x} = k_{-1x}/k_{1x}$, $K_{2x} = k_{-2x}/k_{2x}$, $K_{3x} = k_{-3x}/k_{3x}$; $x = \alpha$, β, or γ). This suggests that the bulk concentrations of R–$(COOH)_2$, (COOH)(COO^-), and R–$(COO^-)_2$ are related to the individual surface concentration of camphoric acid, although the individual surface concentration has not been yet been directly determined.

The experimental results using AFM suggest that the amount and state of adsorbed molecules at the air/water interface for 60 mM camphoric acid solution at pH 10.0 (Fig. 4(c)) are different from those for 20 mM at pH 10.0 (Fig. 4(b)) and 60 mM at pH 11.9 (Fig. 4(d)). That is, the surface concentration of surface active R–$(COOH)_2$, which tends to be adsorbed at the air/water interface, will be significantly higher than those in Fig. 4(b) and (d) since the bulk concentration of R–$(COOH)_2$ in Fig. 4(c) is significantly higher than those in Fig. 4(b) and (c), as indicated in Fig. 2 and 3. In contrast, the surface concentrations of R–$(COOH)_2$ in Fig. 4(b) and (d) are very low. Especially, the existence of surface inactive R–$(COO^-)_2$ in Fig. 4(d) is very high, even with the same concentration of camphoric acid as Fig. 4(c). Thus, the amount of adsorbed molecules on the mica surface in Fig. 4(c) is larger in Fig. 4(b) and (d). The existence of a critical concentration for the surface tension (20 mM in Fig. 2(b) and 35 mM in Fig. 2(c)) has also been discussed for other membrane systems that exhibit oscillatory phenomena.[34–36]

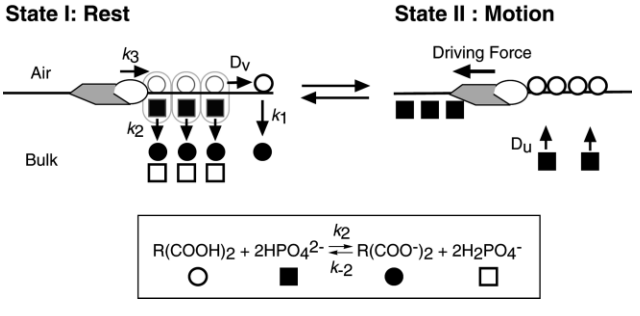

Fig. 6 Schematic representation of the mechanism of the intermittent motion of a camphoric acid boat. States I and II correspond to rest without a driving force and motion driven by the surface tension, respectively. The kinetic parameters are defined in eqn. (4) and (5).

As for the mode change from uniform motion to intermittent motion (Fig. 5(a)), the pH at the aqueous surface changes from acid to neutral with the addition of NH_3, and the surface active R–$(COOH)_2$ is then partly dissolved into the bulk phase. Upon the mode change from intermittent motion to uniform motion (Fig. 5(b)), the pH at the aqueous surface changes from neutral to acid with the addition of HCl. Fig. 5(c) suggests that the self-motion of a camphoric acid boat is variably sensitive to external stimuli. The intermittent motion changed to no motion with the addition of NH_3 due to the pH change to alkaline. No motion reverted to intermittent motion with the addition of HCl due to the surface neutralization. However, further change to the uniform motion was not observed with the addition of HCl since the pH remained almost at 7.0 due to the buffer capacity, as indicated with the pH indicator. The negative velocity seen when the boat passes around the HCl stimulus may be explained as follows (Fig. 5(c)). Before the addition of HCl, R–$(COOH)_2$ develops from the solid scraping and then dissolves as R–$(COO^-)_2$ with the addition of NH_3. R–$(COO^-)_2$ at the aqueous surface of the head of the boat may change to R–$(COOH)_2$ with the addition of HCl, and the surface tension at the head of the boat then decreases. Thus, the negative velocity is generated due to $\gamma_h < \gamma_r$ (γ_h being the surface tension at the head of the boat, and γ_r that at the rear of the boat). These experimental results regarding the responses to chemical stimuli suggest that the mode of self-motion can change reversibly and in different ways depending on the chemical stimuli.

4.2. Numerical simulation of the mode-change in the self-motion due to the chemical environment

To mathematically appreciate the motion of a camphoric acid boat depending on the concentration of phosphate ions, we introduce a mathematical model for a camphoric acid boat in a linear cell. First, we assume that the camphoric acid grain is a material particle because of its sufficiently small volume, and we also approximate the camphoric acid boat as two rigid material particles:

$$(x_1(t), x_2(t)) = (x_c(t) + l, x_c(t) - l) \tag{1}$$

were $x_1(t)$, $x_2(t)$, and $x_c(t)$ denote the front of the plastic boat without camphoric acid, the rear of the plastic boat with camphoric acid, and the center, respectively. $2l$ is the length of the plastic boat. The motion of the camphoric acid boat may then be expressed by the following Newtonian equation:[28,29]

$$\rho\ddot{x}_c(t) = \frac{1}{2}\sum_{i=1}^{2}\frac{\partial}{\partial x}\gamma(u(x_i(t),t)) - \mu\dot{x}_c(t) + \frac{1}{2}\sum_{i=1}^{2} e_i\left(\frac{\partial}{\partial x}\gamma(u(x_i(t),t))\right)^2\dot{x}_c(t), \tag{2}$$

where γ(N m^{-1}) is the surface tension at the air/water interface, $u(x, t)$ (mol m^{-2}) is the surface concentration of the camphoric acid layer diffused from the grain, ρ(kg m^{-2}) is the surface density of the camphoric acid boat, μ(kg m^{-2} s^{-1}) is a constant for the surface viscosity, and e_i (m s N^{-1}) is a coefficient for the term for convection flow, which may be effective as a negative resistance term.[27] Based on the experimental result (Fig. 2(a)) and the general relationship between surface tension and the concentration of a surfactant,[33] the surface

tension may be expressed as a function of $u(x, t)$, as follows:

$$\gamma(u) = \begin{cases} \gamma_0, & 0 \le u \le u_1, \\ a(u-u_1)^2 + \gamma_0, & u_1 < u \le u_2, \\ b(u-u_3)^2 + \gamma_1, & u_2 < u \le u_3, \\ \gamma_1, & u > u_3, \end{cases} \quad (3)$$

where $a = -\gamma_0 - \gamma_1/(u_2 - u_1)(u_3 - u_1)$ and $b = \gamma_0 - \gamma_1/(u_3 - u_2)(u_3 - u_1)$. γ_0 (N m^{-1}) is the surface tension of water and γ_1 (N m^{-1}) ($< \gamma_0$) is the minimum surface tension of water depending on the concentration of the camphoric acid layer.

We next consider a model for the surface concentration of the camphoric acid layer and the concentration of the phosphate ion. The camphoric acid molecule is ionized with phosphate ions around the air/water interface, as indicated in Fig. 6. Therefore, we may obtain the following reaction diffusion equations:

$$\begin{cases} \dfrac{\partial u}{\partial t} = D_u \dfrac{\partial^2 u}{\partial x^2} - k_1 u - k_2 u v^2 + F(x, x_2(t); r_0), \\ \dfrac{\partial v}{\partial t} = D_v \dfrac{\partial^2 v}{\partial x^2} - 2k_2 u v^2, \end{cases} \quad t > 0,\ x \in (0, L), \quad (4)$$

where u (mol m^{-2}) is the surface concentration of R(COOH)$_2$ at the air/water interface, v (mol m^{-2}) is the concentration of HPO_4^{2-} near the air/water interface, D_u (m^2 s^{-1}) is the diffusion coefficient of the camphoric acid layer diffused to the air/water interface, D_v is the diffusion coefficient of HPO_4^{2-}, k_1 (s^{-1}) and k_2 (m^6 mol^{-2} s^{-1}) are the rate constants of dissolution and reaction, respectively, r_0 (m) is the radius of the camphoric acid grain, and L (m) is the length of the water bath. The function F (mol m^{-2} s^{-1}) reflects the development of the camphoric acid layer from the camphoric acid grain to the air/water interface. Although we approximate the camphoric acid grain as a material point in eqn. (2), we introduce a radius of the camphoric acid grain to consider the dependence on the size of the camphoric acid grain. Therefore, function F is defined as follows:

$$F(x, x_2(t); r_0) = \begin{cases} k_3 S_0, & |x - x_2(t)| \le r_0, \\ 0, & |x - x_2(t)| > r_0, \end{cases} \quad (5)$$

where S_0 is the constant amount to be supplied by the camphoric acid grain and k_3 is the rate of diffusion of the camphor layer from the camphoric acid grain. We assume that the decrease in mass of the camphoric acid grain by diffusion of the camphor layer is negligible, *i.e.*, the mass of the grain is constant.

As a boundary condition, we take the following non-flux conditions:

$$\frac{\partial}{\partial x} u(0, t) = \frac{\partial}{\partial x} u(L, t) = 0, \quad \frac{\partial}{\partial x} v(0, t) = \frac{\partial}{\partial x} v(L, t) = 0. \quad (6)$$

To investigate the dependence on the concentration of HPO_4^{2-}, we use the following initial conditions:

$$\begin{cases} u(x, 0) \equiv 0, & v(x, 0) \equiv v_0, \\ x_c(0) = x_A, & \dot{x}_c(0) = x_B. \end{cases} \quad (7)$$

where v_0 is the initial concentration of HPO_4^{2-}.

Finally, we require that $u(\cdot, t)$ is a continuously differentiable function on $(0, L)$.

We now turn to the normalization of eqn.(2)–(7). Let us introduce the following dimensionless parameters and variables, *i.e.*, $\tau = k_3 t$, $y = \sqrt{k_3/D_u}\, x$, $y_k = \sqrt{k_3/D_u}\, x_k (k = 1, 2,$ or c), $U = u/S_0$, $V = v/S_0$, $D = D_v/D_u$, $\hat{\mu} = \mu/\rho k_3$, $E_i = e_i D_u \rho\, k_3^2$ ($i = 1$ or 2), $\hat{l} = \sqrt{k_3/D_u}\, l$, $\Gamma_0 = \gamma_0/(D_u \rho\, k_3^2)$, $\Gamma_1 = \gamma_1/(D_u \rho\, k_3^2)$, $K_1 = k_1/k_3$, $K_2 = (k_2/k_3) v_0^2$, and $K_3 = 2(k_2/k_3) v_0 S_0$.

Rewriting τ, y, $y_k (k = 1, 2,$ or 3), $\hat{\mu}$, $\hat{l}$, and $L_y = \sqrt{k_3/D_u} L$ as t, x, $x_k (k = 1, 2,$ or 3), μ, l, and L, respectively, we derive the following dimensionless model equation:

$$\begin{cases} \ddot{x}_c(t) = \dfrac{1}{2}\displaystyle\sum_{i=1}^{2} \frac{\partial}{\partial x} \Gamma(U(x_i(t), t)) \\ \qquad\qquad -\mu \dot{x}_c(t) + \dfrac{1}{2}\displaystyle\sum_{i=1}^{2} E_i \left(\frac{\partial}{\partial x} \Gamma(U(x_i(t), t)) \right)^2 \dot{x}_c(t), \quad t > 0 \\ \dfrac{\partial U}{\partial t} = \dfrac{\partial^2 U}{\partial x^2} - K_1 U - K_2 U V^2 + F(x, x_2(t); R_0) \\ \qquad\qquad t > 0, x \in (0, L) \\ \dfrac{\partial U}{\partial t} = D \dfrac{\partial^2 V}{\partial x^2} - K_3 U V^2, \end{cases} \quad (8)$$

with initial conditions

$$\begin{cases} U(x, 0) \equiv 0, & V(x, 0) \equiv 1, \\ x_c(0) = x_A, & \dot{x}_c(0) = x_B, \end{cases} \quad (9)$$

and boundary conditions

$$\begin{aligned} \frac{\partial}{\partial x} U(0, t) &= \frac{\partial}{\partial x} U(L, t) = 0, \\ \frac{\partial}{\partial x} V(0, t) &= \frac{\partial}{\partial x} V(L, t) = 0, \end{aligned} \quad (10)$$

where $\Gamma(U)$ and $F(x, x_2; R_0)$ are expressed as

$$\Gamma(U) = \begin{cases} \Gamma_0, & 0 \le U \le U_1, \\ A(U - U_1)^2 + \Gamma_0, & U_1 < U \le U_2, \\ B(U - U_3)^2 + \Gamma_1, & U_2 < U \le U_3, \\ \Gamma_1, & U > U_3, \end{cases} \quad (11)$$

and

$$F(x, x_2; R_0) = \begin{cases} 1, & |x - x_2| \le R_0, \\ 0, & |x - x_2| > R_0. \end{cases} \quad (12)$$

By using dimensionless parameters, $R_0 = \sqrt{k_3/D_u}\, r_0$, $U_j = u_j/S_0$ ($j = 1,$ 2, or 3), $A = (\Gamma_1 - \Gamma_0)/\{(U_2 - U_1)(U_3 - U_1)\}$, and $B = (\Gamma_1 - \Gamma_0)/\{(U_3 - U_2)(U_3 - U_1)\}$. We can perform our numerical simulation based on this dimensionless system (eqn. (8)). However, we record the value of v_0 instead of K_2 and K_3 for the convenience of researchers. We assume that D is very small because the surface diffusion of the camphoric acid layer is significantly greater than the diffusion of phosphate ion in the bulk phase.

Fig. 7 shows a computer simulation of the temporal change in the camphoric acid boat at different v_0. An increase in v_0 corresponds to an increase in the pH of the bulk phase experimentally. When v_0 is small, the boat moves at a constant velocity (Fig. 7(a)). With an increase in v_0, uniform motion changes to intermittent motion *via* oscillatory motion, and the period increases (Fig. 7(b) and (c)). These results suggest that the boat changes from uniform motion to oscillatory motion by Hopf bifurcation when v_0 increases.

Finally, we can explain the mechanism for intermittent motion of the camphoric acid boat using eqn. (8) and (11). If v_0 is very large, the decreasing term, $-K_2 U V^2$, is much larger than the increasing term, F, since $K_2 \gg 1$. Therefore, $\partial\Gamma(U)/\partial x = 0$ in eqn. (8) from eqn. (11) because U cannot increase. As a result, the boat does not move (State I). However, $-K_2 U V^2$ becomes less than 1 as V gradually decreases from 1 to 0 due to $-K_3 U V^2$ in eqn. (8). Hence, U increases due to F, *i.e.*, a camphoric acid layer can accumulate at the water surface. Accordingly, $\partial\Gamma(U)/\partial x \neq 0$ is obtained and therefore the camphoric acid boat moves to another point with $V \equiv 1$ (State II). Thus, intermittent oscillatory motion occurs by repetition

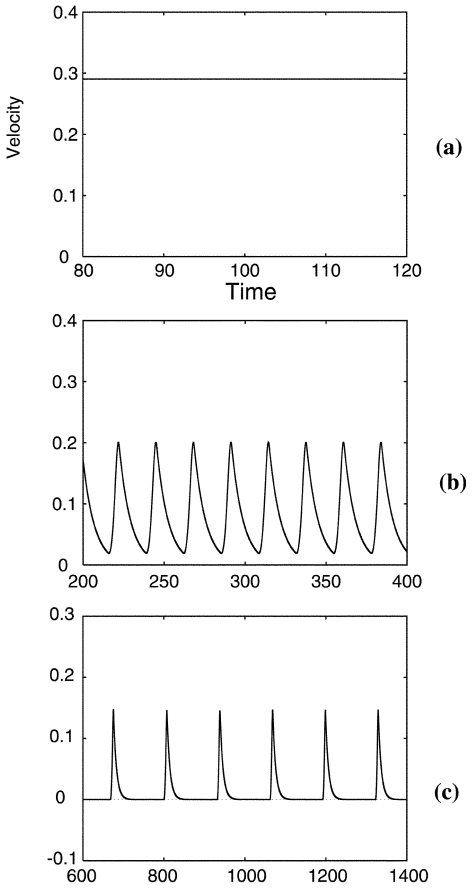

Fig. 7 Time variation of the velocity of a camphoric acid boat at $x_c(t)$. (a) $v_0 = 1$, (b) $v_0 = 20$, and (c) $v_0 = 150$. The fixed parameters in (a), (b), and (c) are $\mu = 0.1$, $E_i = 1.0$, $l = 1.0$, $R_0 = 0.7$, $D = 10^{-4}$, $K_1 = 0.5$, $k_2 = 1.0$, $k_3 = 1.0$, $S_0 = 0.6$, $U_1 = 0.05$, $U_2 = 0.2$, $U_3 = 0.8$, $\Gamma_0 = 1.0$, and $\Gamma_1 = 0.5$.

of States I and II. Thus, the model equations qualitatively reflect the experimental results.

5. Conclusion

The characteristic spontaneous pH-dependent motion may be induced by a change in the state of the camphoric acid layer, which is related to the surface tension, which in turn depends on the concentration of phosphate ion and pH. The nature of the self-motion changes reversibly with the addition of chemical stimuli to the air/aqueous interface. In a future study, a solutocapillary effect (or solute-Marangoni effect) which involves surface convection from low to high surface tension, should be taken into account as an important factor in the camphor motion in addition to the effect of the surface tension gradient.[37,38] In addition, we should measure the Reynolds number in the present system to clarify the effect of the viscous resistance.[22]

According to the Curie–Prigogine theorem, scalar variables cannot couple with vector values under isotropic conditions.[39–41] This implies that a chemo-mechanical transducer can be created under anisotropic conditions. In this experiment, the direction of self-motion was determined by how the camphoric acid scraping was attached to the plastic boat, i.e., the symmetric diffusion of the camphoric acid layer around the scraping is disturbed by the plastic boat. The present study suggests that we may be able to create various manners of self-motion that are sensitive to the environment and to change their vector and mode by considering the concentration *vs.* surface tension relationship and by introducing heterogeneous conditions to the reaction field.

Appendix

Here, we explain how to obtain the curves in Fig. 3. The equilibrium between states α and β is given by eqn. (13).

$$\mathrm{p}K_{\mathrm{a}1} = 4.57 = -\log(C_\beta/C_\alpha) \tag{13}$$

The equilibrium between states β and γ is given by eqn. (14).

$$\mathrm{p}K_{\mathrm{a}2} = 5.10 = -\log(C_\gamma/C_\beta) \tag{14}$$

The total concentration of camphoric acid, C, is the sum of the individual concentrations for the states α, β and γ as described in eqn. (15).

$$C = C_\alpha + C_\beta + C_\gamma \tag{15}$$

The curves in Fig. 3 are obtained based on eqn. (13)–(15).

Acknowledgement

We thank Prof. Masayasu Mimura (Hiroshima University, Japan) for his helpful suggestion on the mathematical modeling. The present study was supported by a Grant-in-Aid for Scientific Research from the Ministry of Education, Science, and Culture of Japan, the Yamada Science Foundation, and the President Fellowship of Nara University of Education.

References

1 R. Yoshida, T. Takahashi, T. Yamaguchi and H. Ichijo, *J. Am. Chem. Soc.*, 1996, **118**, 5134.
2 R. Yoshida, M. Tanaka, S. Onodera, T. Yamaguchi and E. Kokufuta, *J. Phys. Chem. A*, 2000, **104**, 7549.
3 M. Dupeyrat and E. Nakache, *Bioelectrochem. Bioenerg.*, 1978, **5**, 134.
4 S. Kai, E. Ooishi and M. Imasaki, *J. Phys. Soc. Jpn.*, 1985, **54**, 1274.
5 T. Yamaguchi and T. Shinbo, *Chem. Lett.*, 1989, 935.
6 K. D. Barton and R. S. Subramanian, *J. Colloid Interface Sci.*, 1989, **133**, 211.
7 M. K. Chaudhury and G. M. Whitsides, *Science*, 1992, **256**, 1539.
8 F. Brochard, *Langmuir*, 1989, **5**, 432.
9 N. Magome and K. Yoshikawa, *J. Phys. Chem.*, 1996, **100**, 19102.
10 L. E. Scriven and C. V. Sternling, *Nature*, 1960, **187**, 186.
11 Yu. Yu. Stoilov, *Langmuir*, 1998, **14**, 5685.
12 Yu. Yu. Stoilov, *Phys. Uspekhi*, 2000, **43**, 39.
13 C. Bain, G. Burnett-Hall and R. Montgomerie, *Nature*, 1994, **372**, 414.
14 F. Domingues dos Santos and T. Ondarçuhu, *Phys. Rev. Lett.*, 1995, **75**, 2972.
15 S. Nakata, H. Komoto, K. Hayashi and M. Menzinger, *J. Phys. Chem. B*, 2000, **104**, 3589.
16 I. Z. Steinberg, A. Oplatka and A. Katchalsky, *Nature*, 1966, **210**, 568.
17 P. G. Gennes, *Physica A*, 1998, **249**, 196.
18 F. Jülicher, A. Ajdari and J. Prost, *Rev. Mod. Phys.*, 1997, **69**, 1269.
19 R. D. Astumian and M. Bier, *Phys. Rev. Lett.*, 1994, **72**, 1766.
20 K. Sekimoto, *Prog. Theor. Phys.*, 1998, **130**, 17.
21 K. Yoshikawa and H. Noguchi, *Chem. Phys. Lett.*, 1999, **303**, 10.
22 M. Shanahan, *Pour la Science*, 1998, No. 24 (February), p. 106.
23 L. Rayleigh, *Proc. R. Soc. London*, 1890, **47**, 364.
24 S. Nakata, Y. Iguchi, S. Ose, M. Kuboyama, T. Ishii and K. Yoshikawa, *Langmuir*, 1997, **13**, 4454.
25 S. Nakata and Y. Hayashima, *J. Chem. Soc., Faraday Trans.*, 1998, **94**, 3655.
26 S. Nakata, M. I. Kohira and Y. Hayashima, *Chem. Phys. Lett.*, 2000, **322**, 419.
27 S. Nakata, Y. Hayashima and H. Komoto, *Phys. Chem. Chem. Phys.*, 2000, **2**, 2395.

28 Y. Hayashima, M. Nagayama and S. Nakata, *J. Phys. Chem. B*, 2001, **105**, 5353.
29 M. I. Kohira, Y. Hayashima, M. Nagayama and S. Nakata, *Langmuir*, 2001, **17**, 7124.
30 S. Nakata, Y. Iguchi, S. Ose and T. Ishii, *J. Phys. Chem. B*, 1998, **102**, 7425.
31 S. Nakata and Y. Hayashima, *Langmuir*, 1999, **15**, 1872.
32 S. Nakata, Y. Hayashima and T. Ishii, *Colloid. Surf. A*, 2001, **182**, 231.
33 I. Langmuir, *J. Am. Chem. Soc.*, 1917, **39**, 1848.
34 K. Yoshikawa, M. Makino, S. Nakata and T. Ishii, *Thin Solid Films*, 1989, **180**, 117.
35 K. Yoshikawa, M. Shoji, S. Nakata, S. Maeda and H. Kawakami, *Langmuir*, 1988, **4**, 759.
36 K. Yoshikawa and M. Makino, *Chem. Phys. Lett.*, 1989, **160**, 623.
37 V. G. Levich, *Physicochemical Hydrodynamics*, ed. D. B. Spalding, Advance Publications Limited, London, 1977.
38 L. D. Landau and E. M. Lifshits, *Fluid Mechanics*, Pergamon Press, London, 2nd edn., 1987.
39 A. Katchalsky and P. F. Curie, *Nonequilibrium Thermodynamics in Biophysics*, Harvard University Press, Cambridge MA, 1965.
40 I. Prigogine, *Introduction to the Thermodynamics of Irreversible Processes*, Wiley, New York, 2nd edn., 1961.
41 N. Boccara, *Symmetries and Broken Symmetries in Condensed Matter Physics*, IDSET, Paris, 1981.